

Phase separation analysis in the ternary system of poly (butylene succinate) /1,1,2,2,-tetrachloethane/non-solvent in relation to membrane formation

M. Ebrahimpour^{1*}, A. A. Safekordi¹, S. M. Mousavi², A. Heydari Nasab²

¹Department of Chemical Engineering, Science and Research Branch, Islamic Azad University, Tehran, Iran

² Department of Chemical Engineering, Faculty of Engineering, Ferdowsi University of Mashhad, Mashhad, Iran

Submitted December 1, 2016; Accepted August 21, 2017

Phase separation analysis of a three-component, membrane-forming system: poly (butylene succinate) (PBS)/1,1,2,2-Tetrachloethane/ non-solvent is described. Cloud point data were obtained by the titration method on the ternary system diagram from a limited number of experiments. These curves obtained for the different non-solvents including methanol, methanol/isopropanol (50/50,v/v), isopropanol. The phase diagram for a ternary system of poly (butylene succinate) (PBS)/ 1,1,2,2-Tetrachloethane/ non-solvent was determined by numerical calculation on the basis of the Compressible Regular Solution (CRS) model by pure component properties such as, solubility parameter, coefficient of thermal expansion and hard-core volume. In this respect, the binodal curve, spinodal curve and the critical point were determined by numerical calculations. Properties of components that were needed for these calculations have been taken from available data in the literature. The good agreement between the theoretical binodal and experimental cloud points indicates that this model is a promising method to calculate the theoretical phase diagram for membrane forming systems, with particular attention to the fact that no adjustable parameters such as binary interaction parameters should be used for theoretical calculations. Also the cloud point curves obtained for the above non-solvents indicated that methanol has the strongest coagulation power among them. Results show that the composition of the coagulation bath governs effectively the structure of the membranes.

Keywords: binodal curve, cloud point, ternary systems, membranes

INTRODUCTION

Non-solvent Induced Phase Separation (NIPS) is the most popular method for membrane fabrication in which the polymer solution is immersed in a coagulation bath and solvent/ non-solvent exchange occurs between the polymer solution and the bath. The intrusion of non-solvent reduces the thermodynamic stability of the polymer solution, leading to the phase separation that resolves into two phases, i.e. polymer-rich and polymer-lean. From the former phase a continuous polymer matrix is formed, while from the latter, a void structure is formed [1]. This process is controlled by diffusion kinetics and thermodynamic properties of the system. Knowledge of the thermodynamics of the system gives absolutely essential insight into the membrane structures possibly obtained by a particular system [2]. Figure 1 shows the ternary phase diagram for the NIPS process in membrane formation. The line with points A, B, C, and D denotes the path that the membrane takes during this process. At point A, phase inversion has not begun, and the casting solution only consists of solvent, polymer, and additives. At point B, solvent precipitates out and non-solvent molecules take its place. At point C, the membrane begins to solidify, and at point D, the process is complete [3].

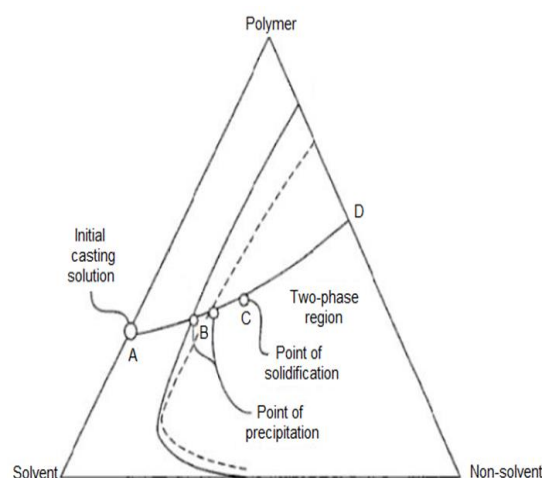


Figure 1. Ternary phase diagram for the phase inversion process through NIPS process [3].

The thermodynamic aspect of membrane formation often involves calculation of a phase diagram using the Flory-Huggins theory, which is usually through calculations of the binodal and spinodal boundaries [4-6]. Up to present, models of higher accuracy but with more complexity, have been developed as alternatives to the Flory-Huggins model [7,8] to predict the thermodynamic behavior

To whom all correspondence should be sent.
E-mail: melika_ebrahimpour2001@yahoo.com

of polymer solutions. The interaction parameters in the Flory-Huggins model are usually determined experimentally which limit its predictive capability, especially for the systems that have not been studied experimentally. In addition, the precise determination of these parameters is of great importance since they have considerable effects on the size and location of the miscibility gap in a ternary phase diagram [9,10]. Recently, some researchers [11-14] have developed a compressible regular solution (CRS) model to explain the phase behavior of polymer blends as well as multicomponent polymer mixtures. This model is in fact an extension of the classical regular solution model to account for compressibility. Thus, in derivation of the expression for free energy of mixing, the free volumes of the constituting components are taken into account [13]. As a result of these researches the calculated binodal curve by this model was further compared with the experimental cloud point measurements. To the authors' best knowledge, no thorough research has been done on the phase separation behavior of a PBS/1,1,2,2-Tetrachloroethane/ non-solvent system. The main goal of this study is to propose a reliable method for phase diagram prediction of PBS membrane forming systems. In this respect, the phase behaviour of a PBS/1,1,2,2-Tetrachloroethane/ non-solvent ternary system has been determined using CRS model. For the ternary systems studied here the phase diagrams including binodal curve, spinodal curve and critical point were calculated. In order to investigate the phase behaviour experimentally, cloud point measurement was carried out, as well. For this purpose, three different compounds were chosen as the non-solvents for the PBS/1,1,2,2- Tetrachloroethane solution.

EXPERIMENTAL

Materials

Poly (butylene succinate) (d: 1.3g/ml at 25°C) was purchased from Sigma-Aldrich. Analytical grade and high purity 1,1,2,2-Tetrachloroethane was supplied from SAMCHUN (Korea) and was used as the solvent. Methanol with a purity of 99.8 wt. % from QRec, isopropanol with a purity of 96 wt. % from Merck were used without further purification as non-solvents. All experiments were performed at a constant temperature of 25°C.

Cloud-point curve determination

The phase diagram of the PBS/1,1,2,2-Tetrachloroethane/ non-solvent combination systems was determined by cloud point measurement. Hence, the ternary phase diagram (cloud- point curve) was obtained by the following

method: PBS solutions with different compositions were placed in glass-ware reactor under stirring and the non-solvent was slowly added to the PBS solutions until the clear solutions remain milky-like. For this purpose, starting polymer solutions with different concentrations (below 20 wt%) in tetrachloroethane were carried out in the glass-ware reactor to achieve homogeneous polymer solutions, these mixtures were stirred by a magnetic stirrer. The ternary phase diagram was obtained from the turbid points. To reach the turbid point, non-solvent was added slowly into the polymer solution under stirring. During titration, the solution temperature was controlled at 25°C with water bath and the addition of 1,1,2,2- Tetrachloroethane was continued until the clear polymer solution visually turned to look milky-like. After, the observation of the first sign of turbidity, addition of non-solvent was stopped and the solution was stirred for an additional 20-40 min to see whether the turbid solution changes to a clear solution or not. If the solution turned to a clear solution, more non-solvent was added, otherwise the determined point was considered as the onset of real turbid point. The ternary composition of turbid point was then calculated from the amount of non-solvent, solvent and polymer present in the glass-ware.

Membrane formation

The PBS asymmetric membrane was prepared using phase inversion method [15]. The polymer dope solution (16 wt.% in 1,1,2,2-Tetrachloroethane) was casted onto a glass plate using a film applicator at 25°C and the evaporation time was 30 second. The glass plate was subsequently immersed in a gelation bath consisting of non-solvent at room temperature. It was then rinsed in distilled water to remove residual solvent.

Morphology of the membranes

Scanning electron microscopy (SEM) was used to observe the morphology of PBS membranes. Top surface and cross-section images were prepared by fracturing the dried membranes in liquid nitrogen and then were coated with gold to provide electrical conductivity. The top and bottom Snapshots of membranes were taken on a KYKY EM3200 scanning electron microscope (SEM). Significant views of surfaces and cross sections were recorded.

RESULTS AND DISCUSSION

Cloud-point data

Figure 2 shows the cloud point curves for the PBS/1,1,2,2- Tetrachloroethane/ non-solvent system that drawn on the triangular diagram over an extended range of polymer concentrations for different non-solvents. The experimental binodal

curve denoting the border between the compositions that were completely stable, metastable, or unstable. Methanol, methanol/isopropanol (50/50, v/v) and isopropanol were used as the non-solvents for the PBS/1,1,2,2-Tetrachloroethane system while the concentration of polymer solution was changed. The closer the cloud point curve to the polymer solvent axis is the stronger non-solvent. Hence, according to Figure 2, the coagulation power of the non-solvents

is in the order of: Methanol > Methanol/isopropanol (50/50, v/v) > isopropanol. As the coagulation power is known to be a parameter that affects phase separation, the above information can be used for selection of suitable non-solvent, e.g. for delayed demixing, the weakest coagulant such as isopropanol should be used.

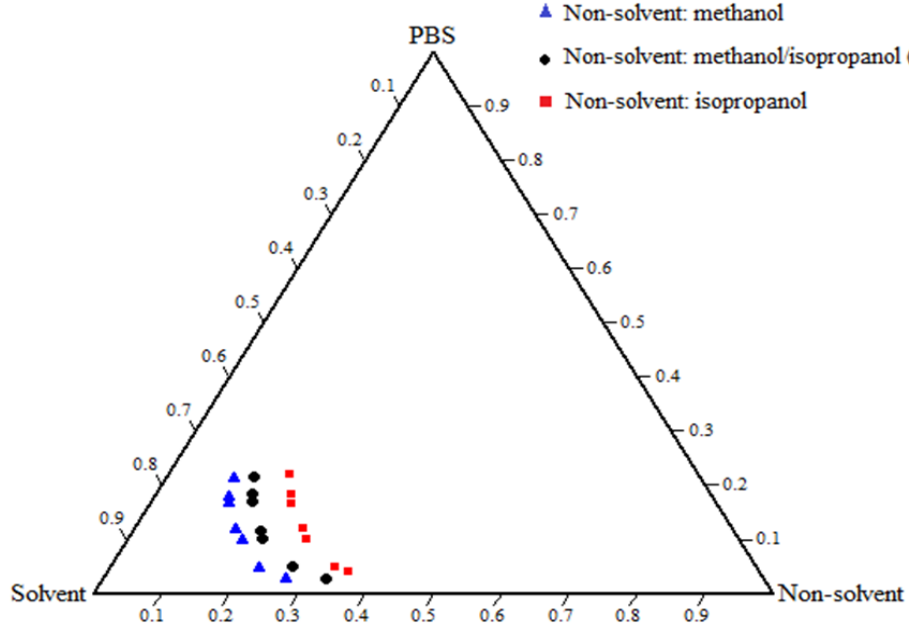


Figure 2. The experimental cloud point data for the PBS/1,1,2,2-tetrachloroethane/ non-solvent ternary system at 25°C.

Binodal curve evaluation

The Gibbs free energy of mixing per unit volume (Δg_{mix}) of a ternary polymer solution in CRS model is defined as follows [16]:

$$\begin{aligned} \Delta g_{mix} &= KT \left(\frac{\varphi_1 \tilde{\rho}_1}{N_1 v_1} \ln(\varphi_1) \right. \\ &+ \frac{\varphi_2 \tilde{\rho}_2}{N_2 v_2} \ln(\varphi_2) + \frac{\varphi_3 \tilde{\rho}_3}{N_3 v_3} \ln(\varphi_3) \left. \right) \\ &+ \varphi_1 \varphi_2 (\tilde{\rho}_1 \delta_{1,0} - \tilde{\rho}_2 \delta_{2,0})^2 \\ &+ \varphi_1 \varphi_3 (\tilde{\rho}_1 \delta_{1,0} - \tilde{\rho}_3 \delta_{3,0})^2 \\ &+ \varphi_2 \varphi_3 (\tilde{\rho}_2 \delta_{2,0} - \tilde{\rho}_3 \delta_{3,0})^2 \end{aligned} \quad (1)$$

The Equation (1) can be separated into compressible and incompressible terms as given in Equation (2):

$$\begin{aligned} \Delta g_{mix} &= KT \left(\frac{\varphi_1 \tilde{\rho}_1}{N_1 v_1} \ln(\varphi_1) \right. \\ &+ \frac{\varphi_2 \tilde{\rho}_2}{N_2 v_2} \ln(\varphi_2) + \frac{\varphi_3 \tilde{\rho}_3}{N_3 v_3} \ln(\varphi_3) \left. \right) \\ &+ \varphi_1 \varphi_2 \tilde{\rho}_1 \tilde{\rho}_2 (\delta_{1,0} - \delta_{2,0})^2 \\ &+ \varphi_1 \varphi_2 (\tilde{\rho}_1 - \tilde{\rho}_2) (\delta_1^2 - \delta_2^2) \\ &+ \varphi_1 \varphi_3 \tilde{\rho}_1 \tilde{\rho}_3 (\delta_{1,0} - \delta_{3,0})^2 \\ &+ \varphi_1 \varphi_3 (\tilde{\rho}_1 - \tilde{\rho}_3) (\delta_1^2 - \delta_3^2) \\ &+ \varphi_2 \varphi_3 \tilde{\rho}_2 \tilde{\rho}_3 (\delta_{2,0} - \delta_{3,0})^2 \\ &+ \varphi_2 \varphi_3 (\tilde{\rho}_2 - \tilde{\rho}_3) (\delta_2^2 - \delta_3^2) \end{aligned} \quad (2)$$

Where φ_i represents the volume fractions with N_i segments of hard-core molar (zero kelvin, zero pressure) volume v_i . The reduced density ($\tilde{\rho}_i$) is given by following Equation:

$$\tilde{\rho}_i = \exp(-\alpha_i T) \quad (3)$$

Where α_i is the volumetric coefficient of thermal expansion. The hard-core solubility parameter, $\delta_{i,0}$, can be calculated by Equation (4):

$$\delta_i^2(T) = \delta_i^2(298) \left(\frac{\rho_i(T)}{\rho_i(298)} \right) \quad (4)$$

In Equation (4), $\delta_i(298)$, is the component solubility parameter at 25 °C which can be calculated from group contribution methods. Also, ρ_i , is the

hard core density of components and given by following Equation [17]:

$$\rho_i = \frac{M_{u,i}}{N_0 v_i} \quad (5)$$

Where $M_{u,i}$ is the segment molecular weight (gr/mol), v_i is hard core volume and N_0 is Avogadro's number.

According to the definition of chemical potential [16], three such equations hold for a ternary polymer solution as follows:

$$\begin{aligned} \frac{\Delta\mu_1}{RT} &= \ln\varphi_1 + 1 - \varphi_1 - \left(\frac{(N_1 v_1)\tilde{\rho}_2}{(N_2 v_2)\tilde{\rho}_1}\right)\varphi_2 \\ &- \left(\frac{(N_1 v_1)\tilde{\rho}_3}{(N_3 v_3)\tilde{\rho}_1}\right)\varphi_3 \\ &+ \left(\frac{(\tilde{\rho}_1\delta_{1,0} - \tilde{\rho}_2\delta_{2,0})^2}{RT}\varphi_2 + \frac{(\tilde{\rho}_1\delta_{1,0} - \tilde{\rho}_3\delta_{3,0})^2}{RT}\varphi_3\right)(\varphi_2 + \varphi_3)V_1 \\ &- \left(\frac{(N_1 v_1)\tilde{\rho}_2}{(N_2 v_2)\tilde{\rho}_1}\right)\left(\frac{(\tilde{\rho}_2\delta_{2,0} - \tilde{\rho}_3\delta_{3,0})^2}{RT}\right)V_2\varphi_2\varphi_3 \quad (6) \end{aligned}$$

$$\begin{aligned} \frac{\Delta\mu_2}{RT} &= \ln\varphi_2 + 1 - \varphi_2 - \left(\frac{(N_2 v_2)\tilde{\rho}_1}{(N_1 v_1)\tilde{\rho}_2}\right)\varphi_1 \\ &- \left(\frac{(N_2 v_2)\tilde{\rho}_3}{(N_3 v_3)\tilde{\rho}_2}\right)\varphi_3 \\ &+ \left(\left(\frac{(N_2 v_2)\tilde{\rho}_1}{(N_1 v_1)\tilde{\rho}_2}\right)\frac{(\tilde{\rho}_1\delta_{1,0} - \tilde{\rho}_2\delta_{2,0})^2}{RT}V_1\varphi_1 + \frac{(\tilde{\rho}_2\delta_{2,0} - \tilde{\rho}_3\delta_{3,0})^2}{RT}V_2\varphi_3\right)(\varphi_1 + \varphi_3) \\ &- \left(\frac{(N_2 v_2)\tilde{\rho}_1}{(N_1 v_1)\tilde{\rho}_2}\right)\left(\frac{(\tilde{\rho}_1\delta_{1,0} - \tilde{\rho}_3\delta_{3,0})^2}{RT}\right)V_1\varphi_1\varphi_3 \quad (7) \end{aligned}$$

$$\begin{aligned} \frac{\Delta\mu_3}{RT} &= \ln\varphi_3 + 1 - \varphi_3 - \left(\frac{(N_3 v_3)\tilde{\rho}_1}{(N_1 v_1)\tilde{\rho}_3}\right)\varphi_1 \\ &- \left(\frac{(N_3 v_3)\tilde{\rho}_2}{(N_2 v_2)\tilde{\rho}_3}\right)\varphi_2 \\ &+ \left(\left(\frac{(N_3 v_3)\tilde{\rho}_1}{(N_1 v_1)\tilde{\rho}_3}\right)\frac{(\tilde{\rho}_1\delta_{1,0} - \tilde{\rho}_3\delta_{3,0})^2}{RT}V_1\varphi_1 + \left(\frac{(N_3 v_3)\tilde{\rho}_2}{(N_2 v_2)\tilde{\rho}_3}\right)\frac{(\tilde{\rho}_2\delta_{2,0} - \tilde{\rho}_3\delta_{3,0})^2}{RT}V_2\varphi_2\right)(\varphi_1 + \varphi_2) \\ &- \left(\frac{(N_3 v_3)\tilde{\rho}_1}{(N_1 v_1)\tilde{\rho}_3}\right)\left(\frac{(\tilde{\rho}_1\delta_{1,0} - \tilde{\rho}_2\delta_{2,0})^2}{RT}\right)V_1\varphi_1 \quad (8) \end{aligned}$$

Where V_i denotes the molar volume of component i , $\Delta\mu_i$ ($i = 1, 2, 3$) is the difference between the chemical potential of component i in the mixture. On the basis of the definition of the binodal curve, the chemical potential of the polymer-rich phase and that of the polymer-lean phase achieve equilibrium. This equilibrium in a membrane forming system consisting of non-solvent (1), solvent (2) and polymer (3) are as follows:

$$\Delta\mu_{i,A} = \Delta\mu_{i,B}, \quad i = 1,2,3 \quad (9)$$

A and B indices denote polymer-lean and polymer-rich phases. In addition, the components in the two phases obey the material conservation Equations [18]:

$$\sum \varphi_{i,A} = \sum \varphi_{i,B} = 1, \quad i = 1,2,3 \quad (10)$$

Equations (6-10) include five coupled nonlinear equations with six unknowns: $\varphi_{1,A}, \varphi_{2,A}, \varphi_{3,A}, \varphi_{1,B}, \varphi_{2,B}$, and $\varphi_{3,B}$. If one of one composition is chosen as an independent value, five non-linear equations are solved simultaneously to determine the unknown variables.

The objective function is as follows [19]:

$$F = \sum f_i^2, \quad (i = 1,2,3) \quad (11)$$

Where f_1, f_2 and f_3 can be calculated as follows:

$$f_1 = \Delta\mu_{1,A} - \Delta\mu_{1,B} \quad (12)$$

$$f_2 = \frac{v_1}{v_2}(\Delta\mu_{2,A} - \Delta\mu_{2,B}) \quad (13)$$

$$f_3 = \frac{v_1}{v_3}(\Delta\mu_{3,A} - \Delta\mu_{3,B}) \quad (14)$$

The amount of PBS in the polymer-lean phase was very small, so we assumed that $\varphi_{3,A}$ was negligible or zero. The initial composition of the polymer-rich phase is supposed to be a point on the ternary phase diagram that is close to the PBS side on the PBS–non-solvent axis, and the initial composition of the polymer-lean phase close to the non-solvent side [20].

The major characteristics of the CRS theory is its capacity to account for free volumes of pure components and the mixture defined as the difference between the total and hard-core volumes. This feature gives it some superiority over the classical Flory-Huggins theory. Another advantage of CRS model is its predictive capability that needs only pure component properties as input variables but it does not estimate or measure any binary or ternary parameters [13].

Spinodal curve evaluation

The spinodal curve can be calculated using following Equation [19]:

$$G_{22}.G_{33} = (G_{23})^2 \quad (15)$$

The Gibbs free energy of mixing for different components resulted by following Equation:

$$G_{ij} = \left(\frac{\partial^2 \Delta \bar{G}_m}{\partial \phi_i \partial \phi_j} \right)_{\phi_{ref}} \quad (16)$$

G_{22} , G_{23} , and G_{33} as free energies can be written as follows:

$$G_{22} = \frac{1}{\phi_1} + \frac{v_1}{v_2 \phi_2} - 2g_{12} + 2(u_1 - u_2) \left(\frac{dg_{12}}{du_2} \right) + u_1 u_2 \left(\frac{d^2 g_{12}}{du_2^2} \right) \quad (17)$$

$$\begin{aligned} G_{23} &= \frac{1}{\phi_1} - (g_{12} + g_{13}) + \frac{v_1}{v_2} g_{23} \\ &+ u_2(u_1 - 2u_2) \left(\frac{dg_{12}}{du_2} \right) + u_1 u_2^2 \left(\frac{d^2 g_{12}}{du_2^2} \right) \\ &- \phi_3 \left(\frac{dg_{13}}{d\phi_3} \right) \\ &+ \frac{v_1}{v_2} \phi_3 \left(\frac{dg_{23}}{d\phi_3} \right) \end{aligned} \quad (18)$$

$$\begin{aligned} G_{33} &= \frac{1}{\phi_1} + \frac{v_1}{v_3 \phi_3} - 2g_{13} - 2u_2^2(1 - u_1) \left(\frac{dg_{12}}{du_2} \right) \\ &+ u_1 u_2^3 \left(\frac{d^2 g_{12}}{du_2^2} \right) + 2(\phi_1 - \phi_3) \left(\frac{dg_{13}}{d\phi_3} \right) \\ &+ \phi_1 \phi_3 \left(\frac{d^2 g_{13}}{d\phi_3^2} \right) + \frac{2v_1}{v_2} \phi_2 \left(\frac{dg_{23}}{d\phi_3} \right) \\ &+ \frac{v_1}{v_2} \phi_3 \phi_2 \left(\frac{d^2 g_{23}}{d\phi_3^2} \right) \end{aligned} \quad (19)$$

By applying Equation (10) with Equations (15-19) and chosen one of the parameters as independent parameter, spinodal curve was obtained. The numerical procedure is the same as that of binodal case.

Critical point evaluation

The position of critical point (the intersection of binodal and spinodal curve) is defined by following Equation [20]:

$$\begin{aligned} 1 - \frac{V_1}{V_2} \left(\frac{\phi_1^c}{\phi_2^c} \right)^2 - 3 \frac{G_{22}}{G_{23}} \left(1 - \frac{G_{22}}{G_{23}} \right) \\ - \left(1 - \frac{V_1}{V_3} \right) \left(\frac{\phi_1^c}{\phi_3^c} \right)^2 \left(\frac{G_{22}}{G_{23}} \right)^3 \\ = 0 \end{aligned} \quad (20)$$

With combining Equation (15) with Equation (20) which are in conjunction with Equation (10) and solving simultaneously of them, the compositions at critical point was calculated.

We used Matlab 7.0 to compute the phase diagram of the PBS/1,1,2,2- Tetrachloroethane/ non-solvent ternary system. The values of the component parameters used for calculation of binodal, spinodal and the critical point are listed in Table 1.

Table 1. Parameters used for numerical calculation [21-24].

	(g/cm^3) ρ	(K^{-1}) α	($\text{J}^{1/3}/\text{cm}^{3/2}$) δ	$N_i v_i$ (cm^3/mol)
PBS	1.3	0.00026	20.2	132.4
1,1,2,2- Tetrachloroethane	1.56	0.00099	20	107.6
methanol	0.796	0.0019	29.2	50.2
isopropanol	0.785	0.00156	23.3	76.5
Methanol/isopropanol(50/50,v/v)	0.792	0.0015	26.2	63.4

Phase diagrams of PBS/1,1,2,2- tetrachloroethane /non-solvent system and membrane structure analysis

Thermodynamic analysis reveals the effect of interaction potentials on the mixing and demixing of blended components, which are often demonstrated by phase diagrams [25].

Figures (3-5) show the ternary phase diagrams of PBS/1,1,2,2- Tetrachloroethane /non-solvent systems at 25 °C, which are constructed based on the

cloud-point measurements, binodal , spinodal and critical point calculations.

These figures reveal that a small amount of methanol as non-solvent (less than 20%) is needed for liquid-liquid phase separation. Thus the membranes are likely to form by instantaneous demixing upon coagulation step and hence it is expected to form a relatively porous top layer that makes it suitable for ultrafiltration and microfiltration applications [9]. Due to the large polar parameter (δ_p) of methanol as non-solvent,

which indicates its high polarity, it can be predicted that this alcohol has appropriate interaction with the polar section of PBS polymer. In addition to this property, the small size of methanol compared with isopropanol (particularly methanol small size) makes a great tendency and ability for penetration in to nascent film in coagulation bath and the exchange process of solvent/non-solvent can be accelerated. Thus, more porous structure of membrane is obtained (Figure 6a1).

Generally, a higher diffusion of a non-solvent (methanol) in a solvent (1,1,2,2- tetrachloroethane)

results in a faster precipitation [25], that may induce delayed solid-liquid demixing during the formation of membrane. Therefore, the liquid-liquid demixing controls the phase separation. However, by introducing isopropanol as non-solvent, the liquid-liquid demixing process is delayed, and the solid-liquid demixing process occurs. Significant finding is that the porosity is slightly decreased when the coagulant component is changed from methanol to methanol/ isopropanol (50/50, v/v) and isopropanol as shown in Figure 6 respectively.

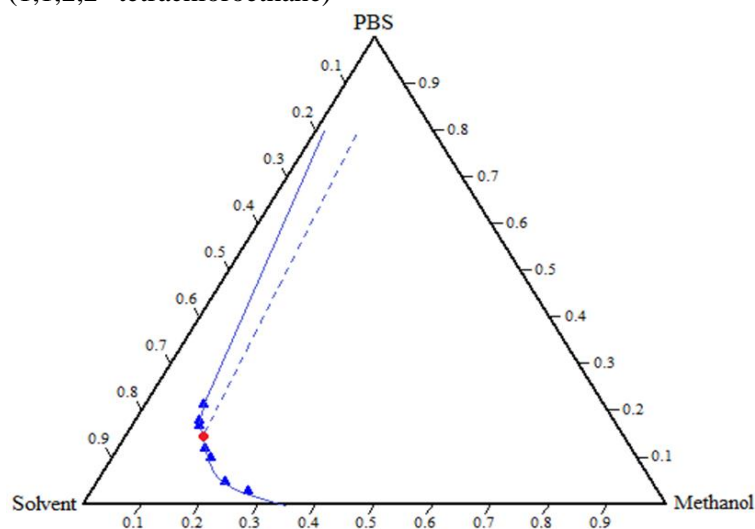


Figure 3. Calculated phase diagram for PBS/1,1,2,2- tetrachloroethane /methanol system at $T = 25^{\circ}\text{C}$, (—) binodal curve, (- - -) spinodal curve, (marker : ▲) experimental cloud point data and (◆) critical point.

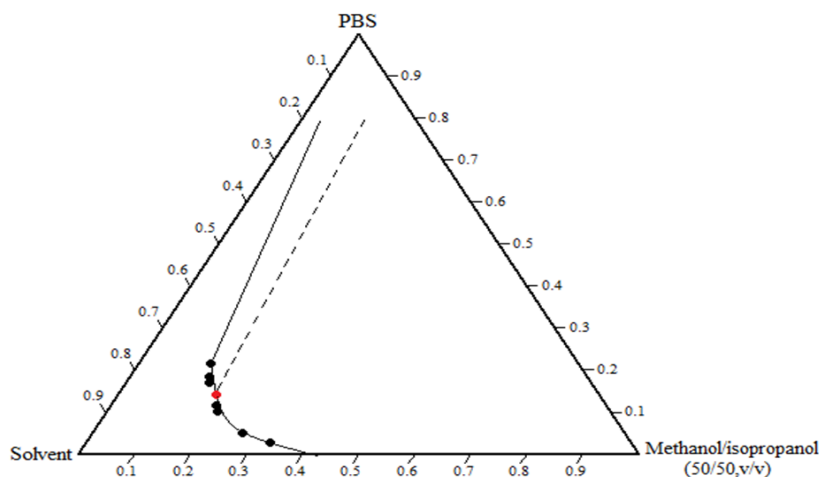


Figure 4. Calculated phase diagram for PBS/1,1,2,2- tetrachloroethane /(methanol/isopropanol (50/50,v/v)) system at $T = 25^{\circ}\text{C}$, (—) binodal curve, (- - -) spinodal curve, (marker : ●) experimental cloud point data and (◆) critical point.

With increasing isopropanol content in the coagulation bath, the phase separation process is eventually dominated by the solid-liquid demixing. So, the closer binodal curve to the polymer solvent axis is obtained when methanol used as non-solvent. These observations are in agreement with the phase diagrams. The calculated binodal curve was further

compared with the experimental cloud point measurements in Figures (3-5). There is a good agreement between experimental data and the theoretical binodal curve, despite the fact that no experimental measurement of model parameters has been done. Also from phase diagrams can be found that methanol has the strongest coagulation power

than others. Since its binodal curve is closer to the PBS-solvent axis on the triangular diagram. The difference in Hansen’s solubility parameters between PBS and the non-solvents is of the order (PBS-methanol) > (PBS-methanol/isopropanol

(50/50, v/v)) > (PBS-isopropanol). A larger difference in solubility parameter with polymer usually implies a shorter time for solid–liquid demixing process to occur.

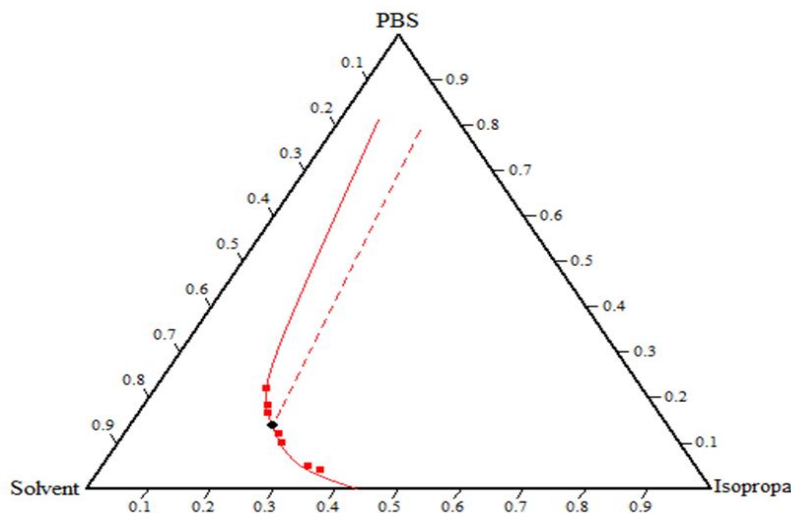


Figure 5. Calculated phase diagram for PBS/1,1,2,2- Tetrachloroethane / isopropanol system at T = 25^oC, (___) binodal curve, (- - -) spinodal curve ,(marker : ■) experimental cloud point data and (●) critical point.

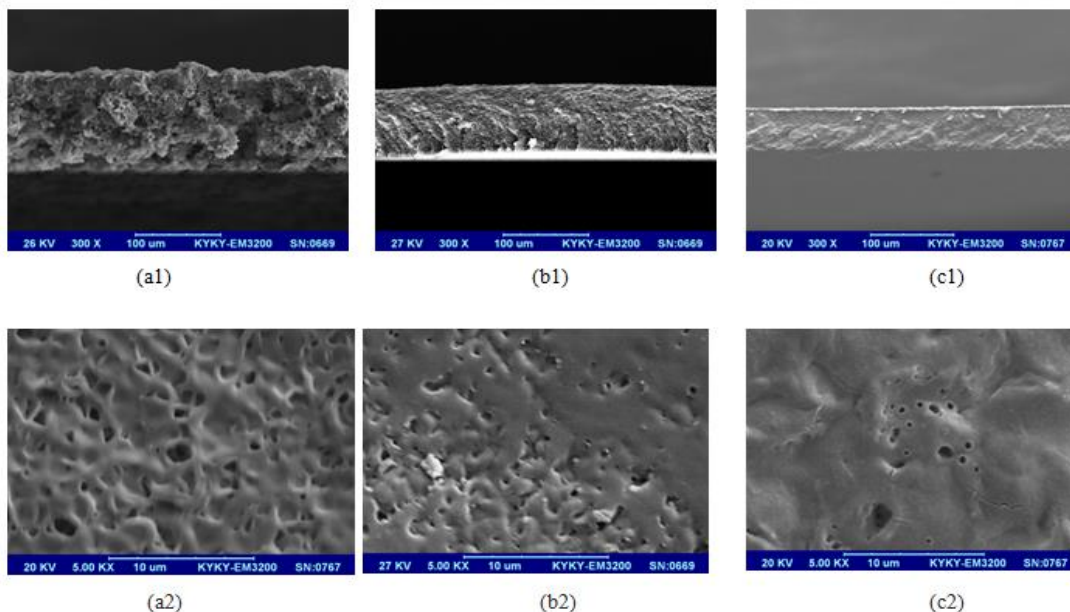


Figure 6. SEM image of PBS membranes: (a1): cross section and (a2): top surface of PBS membrane prepared in methanol coagulation bath, (b1): cross section and (b2): top surface of PBS membrane prepared in methanol/isopropanol (50/50, v/v) coagulation bath, (c1): cross section and (c2): top surface of PBS membrane prepared in isopropanol coagulation bath.

The use of the CRS model has enabled us to calculate the phase diagram of the PBS/1,1,2,2-Tetrachloroethane /non-solvent membrane forming system directly from pure component properties. As can be seen, the general thermodynamic behaviour of the system is relatively well demonstrated. However if we desire to use the Flory-Huggins model to calculate the phase diagram, we would have to measure or estimate the binary interaction

parameters which take more time and possibly accompanied by some errors.

It should be noted here that in spite of its advantages, the CRS model fails to predict the phase behaviour of strong specific interactions such as hydrogen bonding and its predictive capability is limited to weak interaction systems [11].

The composition of the critical point of ternary system is given in Table 2. The critical polymer

composition determines the mechanism of liquid-liquid phase separation. Above the critical point, nucleation of the polymer-lean phase occurs and the polymer-rich phase will form the continuous phase. Therefore, upon membrane production, the composition of the initial casting solution should be selected over the critical polymer composition to ensure sufficient mechanical stability of the membrane [26].

Table 2. The composition of the critical point of ternary systems.

Ternary system	φ_1	φ_2	φ_3
PBS/1,1,2,2-Tetrachloroethane/methanol	0.115	0.715	0.17
PBS/1,1,2,2-Tetrachloroethane/(methanol/isopropanol (50/50,v/v))	0.17	0.667	0.163
PBS/1,1,2,2-Tetrachloroethane/isopropanol	0.21	0.638	0.152

CONCLUSION

The phase separation behavior of polymer solutions is one of the factors that affect the structure of membranes fabricated by the phase separation process. The behavior of polymer solutions during phase inversion further depends on different parameters such as type of polymer, solvent, non-solvent and other additives. In this work, phase separation behavior of the polybutylene succinate casting solution was investigated for different types of non-solvent via cloud point experiments. The following conclusions are drawn from the experimental results:

1. The results suggest that the thermodynamic stability of the PBS/1,1,2,2-tetrachloroethane/non-solvent systems follows the sequence: methanol < methanol/isopropanol (50/50, v/v) isopropanol. Therefore, methanol is a strong non-solvent for the PBS/1, 1, 2, 2-tetrachloroethane system.
2. The CRS model was used to calculate the theoretical phase diagram. A good agreement between experimental measurements and theoretical calculations of ternary systems leads to the conclusion that the model can serve as a promising thermodynamic tool to predict phase behaviour of PBS/1,1,2,2-tetrachloroethane/non-solvent membrane forming systems.
3. The membrane morphology prepared in the methanol coagulation bath presented higher porosity, compared to membranes prepared in the methanol/isopropanol (50/50,v/v) and isopropanol coagulation baths.

Nomenclature

$\Delta\mu_i$	chemical potential difference of component i between the mixture
Δg_{mix}	Gibbs free energy of mixing per unit volume of a ternary polymer mixture (Jmol^{-1})
R	gas constant ($8.314 \text{ J mol}^{-1} \text{ K}^{-1}$)
T	absolute temperature (K)
φ_i	volume fraction of component i
V_i	molar volume of component i
K	Boltzmann constant
$\tilde{\rho}_i$	Reduced density of component i
α_i	volumetric coefficient of thermal expansion
ρ_i	hard-core density
$\delta_i(298)$	component solubility parameter at 25°C
N_i	number of segments in the hard-core volume (v_i) of component i
v_i	volume fraction of component i
$\delta_{i,0}$	hard-core solubility parameter

REFERENCES

1. G.H. Bakeri, A.F. Ismail, M. Rahimnejad, T. Matsuura, *J. Polym. Res.*, **21**, 386 (2014).
2. R.M. Boom, T.H. Van den Boomgaard, J.W. Van den Berg, *C.A. Polymer*, **4**, 2348 (1992).
3. J.Z. Ren, Z.S. Li, F.S. Wong, *J. Membr. Sci.*, **241**, 305. (2004).
4. F.W. Altena, C.A. Smolders, *Macromolecules*, **15**, 1491 (1982).
5. Y.M. Wei, Z.L. Xu, X.T. Yang, H.L. Liu, *Desalination*, **192**,91 (2006).
6. A. Mansourizadeh, A.F. Ismail, *Desalination*, **287**, 220 (2012).
7. I.C. Sanchez, C.G. Panayiotou, Equations of state thermodynamics of polymer and related solutions. Marcel & Dekker, New York, 1994.
8. I.G. Economou, *Ind Eng Cham Res.*, **41**, 953 (2002).
9. Y. Tian, J. Booth, E. Meehan, D.S. Jones, S. Li, G.P. Andrews, *Mol. Pharmaceutics*, **10**, 236 (2013).
10. A. Horta, Statistical thermodynamics of preferential sorption, *Macromolecules* 1979, 12, 785-789.
11. M. Karimi, W. Albrecht, M. Heuchel, M.H. Kish, J. Frahn, T. Weigel, D. Hofmann, H. Modarress. A. Lendlein, *J. Membr. Sci.*, **265**, 1 (2005).
12. J.A. Gonzalez-Leon, A.M. Mayes, *Macromolecules*, **36**, 2508 (2003).
13. Z. Maghsoud, M.H. Navid Famili, S.H. Madaeni, *Iran. Polym. J.*, **19**, 581 (2010).
14. S.S. Madaeni, L. Bakhtiari, E. Salehi, *Polym Adv Technol.*, **24**, 1011 (2013).
15. T. Tanaka, M. Takahashi, S. Kawaguchi, T. Hashimoto, H. Saitoh, T. Kouya, M. Taniguchi, D.R. Lloyd, *Desalination Water Treat.*, **17**, 176 (2010).
16. H. Tompa, *Polymer Solutions*; Butterworths: London, 1956.
17. A.V.G. Ruzette, A.M. Mayes, *Macromolecules*, **34**, 1894 (2001).
18. L. Tan, D. Pan, N. Pan, *J. Appl. Polym. Sci.*, **110**, 3439 (2008).

19. C. Barth, M.C. Gonçalves, A.T.N. Pires, J. Roeder, B.A. Wolf, *J. Membr. Sci.*, **169**, 287 (2000).
20. L. Yilmaz, A.J. McHugh, *J. Appl. Polym. Sci.*, **31**, 997 (1986).
21. K. Raznjevic, Handbook of Thermodynamic Tables and Charts: New York, NY, McGraw-Hill Book Co., 1975, pp 392.
22. J.A. Riddick, W.B. Bunger, T.K. Sakano, Organic Solvents. Physical Properties and Methods of Purification, 4th ed.; New York, NY, John Wiley & Sons, 1986; pp 1325.
23. E. Flick, W. Ethers, Industrial Solvents Handbook, Noyes Data Corporation, New Jersey, 1998. pp 487.
24. D.W. van Krevelen; K. Te Nijenhuis, Properties of Polymers: Their Correlation with Chemical Structure; Their Numerical Estimation and Prediction from Additive Group Contributions, 4th ed.; Elsevier Science, Amsterdam, 2009; 189- 228.
25. P. Sukitpaneevit, T.S. Chung, *J. Membr. Sci.*, **340**, 192 (2009).
26. M. Mulder, Basic Principles of Membrane Technology, Kluwer Academic, Dordrecht, 1996, pp. 81- 156.